Influence of Chloride, Sulfate, and Nitrate Ions in Modified Watts Electrolytes on the Morphology and Corrosion Resistance of Nickel Electrodeposits

Gecilio Pereira da Silva[1] *, Valdessandro Farias Dantas[2], Luiz Ferreira da Silva Filho[3], Zilvam Melo dos Santos[4], Richelly Nayhene de Lima[5], Eduardo Lins de Barros Neto[6]

[1]gecilio@ufersa.edu.br, Engineering Center, Federal Rural University of the Semiarid (UFERSA), Mossoró, Rio Grande do Norte, Brazil. ORCID: https://orcid.org/0009-0003-2806-7792

[2]valdessandro.dantas@gmail.com, Engineering Center, Federal Rural University of the Semiarid (UFERSA), Mossoró, Rio Grande do Norte, Brazil. ORCID: https://orcid.org/0000-0002-5798-355X

[3] luiz.filho@ufersa.edu.br, Engineering Center, Federal Rural University of the Semiarid (UFERSA), Mossoró, Rio Grande do Norte, Brazil. ORCID: https://orcid.org/0009-0008-9701-4324

[4]zilvammelo@ufersa.edu.br, Engineering Center, Federal Rural University of the Semiarid (UFERSA), Mossoró, Rio Grande do Norte, Brazil. ORCID: https://orcid.org/0000-0002-0836-2204

[5]richellylima04@gmail.com, Directorate of people development and quality of life, State University of Rio Grande do Norte (UERN), Mossoró, Rio Grande do Norte, Brazil. ORCID: https://orcid.org/0000-0003-2952-3190

[6]eduardo.lins@ufrn.br[6], Department Of Food Engineering, Federal University Of Rio Grande Do Norte (UFRN), Mossoró, Rio Grande do Norte, Brazil. ORCID: https://orcid.org/0000-0002-1310-7689

* corresponding author

Abstract

Nickel electrodeposits have wide industrial applications due to their resistance, durability, and ability to extend the service life of metallic components. In this study, nickel coatings were obtained from modified Watts baths predominantly containing chloride (ENC), sulfate (ENS), or nitrate (ENN) anions, under constant operational conditions: Ni^{2+} concentration of 1.34 mol·L^{-1}, H_3BO_3 concentration of 0.73 mol·L^{-1}, temperature of 50 °C, pH 4.0, stirring rate of 100 rpm, and electrolysis time of 15 minutes. The influence of these anions on coating morphology, thickness, cathodic current efficiency, and corrosion resistance was evaluated. Surface morphology was examined by Scanning Electron Microscopy (SEM), while electrochemical behavior was assessed by Linear Potentiodynamic Polarization (LPP) and Electrochemical Impedance Spectroscopy (EIS) in a 3.0% NaCl solution, using an AUTOLAB PGSTAT 204. The results indicated that ENC and ENS coatings exhibited greater thickness and higher current efficiency than ENN coatings. Morphologically, ENS deposits showed predominantly nodular structures, ENC coatings exhibited a homogeneous nodular–dendritic morphology, and ENN coatings presented irregular and porous surfaces. Electrochemical analyses revealed that ENS coatings displayed more noble corrosion behavior (Ecorr = –384.0 mV) and higher corrosion resistance, whereas ENN coatings showed inferior performance (Ecorr = –706.0 mV). These findings demonstrate that chloride, sulfate, and nitrate anions significantly affect the morphological and electrochemical properties of nickel electrodeposits.

Keywords: corrosion, electrodeposition, electrochemistry, nickel.

Influência dos íons cloreto, sulfato e nitrato em eletrólitos de Watts modificados na morfologia e resistência à corrosão de eletrodepósitos de níquel

Resumo

Eletrodepósitos de níquel apresentam ampla aplicação industrial devido à sua resistência, durabilidade e capacidade de ampliar a vida útil de componentes metálicos. Neste estudo, eletrodepósitos de níquel foram obtidos a partir de banhos de Watts modificados, contendo predominantemente os ânions cloreto (ENC), sulfato (ENS) ou nitrato (ENN), mantendo-se constantes as condições operacionais: Ni^{2+} na concentração de 1,34 mol·L^{-1}, H_3BO_3 na concentração de 0,73 mol·L^{-1}, temperatura de 50 °C, pH 4,0, taxa de agitação de 100 rpm e tempo de eletrólise de 15 minutos. Avaliou-se a influência desses ânions na morfologia, espessura dos depósitos, rendimento de corrente catódica e resistência à corrosão. As análises morfológicas foram realizadas por Microscopia Eletrônica de Varredura (MEV), e os ensaios eletroquímicos por Polarização Linear Potenciodinâmica (PLP) e Espectroscopia de Impedância Eletroquímica (EIE), em solução aquosa de NaCl 3,0%. ***Os resultados mostraram que os eletrodepósitos ENC e ENS apresentaram maiores espessuras e maior rendimento de corrente em relação aos eletrodepósitos ENN. Morfologicamente, os depósitos ENS exibiram estruturas predominantemente nodulares, os revestimentos ENC apresentaram morfologia nodular–dendrítica homogênea, e os revestimentos ENN apresentaram superfícies irregulares e porosas. Do ponto de vista eletroquímico, os revestimentos ENS exibiram comportamento mais nobre (Ecorr = −384,0 mV) e maior resistência à corrosão, enquanto os revestimentos ENN apresentaram desempenho inferior (Ecorr = −706,0 mV). Conclui-se que os ânions cloreto, sulfato e nitrato afetam significativamente as propriedades morfológicas e eletroquímicas dos eletrodepósitos de níquel.***
Palavras-chave: *corrosão, eletrodeposição, eletroquímica, níquel.*

1 Introduction

Nickel electrodeposits are widely used in industrial applications due to their high hardness, mechanical strength, good ductility, and excellent corrosion resistance (Abbasi-Amandi *et al.*, 2021; Dibari, 2009; Ahmad, 2006). Electrodeposition is one of the most widely used methods for obtaining these coatings, as its operational parameters directly influence their properties, including purity level, phase composition, microstructure, and coating thickness. Among the key variables are electrolyte that govern the electrodeposition process composition, current density, pH, and temperature (Mubshrah *et al.*, 2024; Oliveira *et al.*, 2022; El-Hallag *et al.*, 2021; Wang *et al.*, 2021; Ahmad, 2006; Karayannis; Patermarakis, 1995).

Traditionally, nickel coatings are produced using Watts-type electrolytes, in which the selection of specific nickel salts is justified by the influence that sulfate and chloride anions exert both on the electrolyte behavior and on the properties of the resulting coatings (Chat-Wilk *et al*., 2021; Rusu *et al.*, 2012; Dibari, 2009; Ahmad, 2006; Karayannis; Patermarakis, 1995).

In the literature, references concerning the influence of anions on the electrodeposition process and on the characteristics of nickel electrodeposits are scarce. Therefore, this study aims to evaluate the effect of chloride (Cl^-), sulfate (SO_4^{2-}), and nitrate (NO_3^-) anions in nickel electrolytes on the corrosion resistance of nickel coatings, seeking to contribute to a better understanding of this subject.

This study first presents the theoretical foundations of nickel electrodeposition and electrochemical techniques applied to corrosion studies in Section 2. Section 3 details the experimental methods employed, including Linear Potentiodynamic Polarization (LPP), Electrochemical Impedance Spectroscopy (EIS), and Scanning Electron Microscopy (SEM), to comparatively assess the corrosion resistance of nickel coatings and their respective surface morphologies. The influence of Cl^-, SO_4^{2-}, and NO_3^- anions in the electrolytes on cathodic current efficiency, morphology, and corrosion resistance is presented in Section 4, Results and Discussion.

2 Theoretical reference

2.1 Nickel Electrodeposition

Nickel electrodeposition is a versatile process that enables the production of coatings on various substrates with both decorative and engineering characteristics. These electrodeposits are typically bright, polished, and protective, and are generally synthesized from solutions that deposit pure nickel (Rudnik, 2024; Abbasi-Amandi *et al.*, 2021; Dibari, 2009; Oriňáková, 2006).

During nickel plating, the anode, composed of metallic nickel, gradually dissolves, releasing Ni^{2+} ions into the electrolyte to replenish those consumed during deposition on the substrate. This ensures a stable ion concentration, thereby allowing the electrodeposition to continue efficiently over long durations (Dibari, 2009; Oriňáková, 2006).

Industrial nickel plating baths and their operating conditions are typically based on the Watts formulation. This electrolyte generally contains nickel sulfate (225–410 g L^{-1}), nickel chloride (30–90 g L^{-1}), and boric acid (30–45 g L^{-1}), operating at temperatures between 44 and 71 °C, with pH values ranging from 3.0 to 4.2 and current densities between 1 and 11 A dm^{-2} (Nickel Institute, 2022; Dibari, 2009; Ahmad, 2006). Nickel sulfate acts as the main source of Ni^{2+} ions, while nickel chloride serves as a secondary source, primarily assisting in anode dissolution and enhancing the electrolyte's conductivity. Boric acid helps stabilize the solution's pH and contributes to the formation of ductile, high-quality deposits (Nickel Institute, 2022; Dibari, 2009; Ahmad, 2006; Dennis; Such, 1993).

2.2 Electrochemical Techniques Applied to Corrosion Analysis

Electrochemical methods for corrosion analysis offer high sensitivity and enable the real-time determination of corrosion rates, as well as the evaluation of coating protection and durability. Among the most widely used techniques are Linear Potentiodynamic Polarization (LPP) and Electrochemical Impedance Spectroscopy (EIS). While LPP provides valuable kinetic and quantitative information, it causes a significant perturbation of the system, which may alter the material surface. In contrast, EIS applies only small perturbations, allowing the identification of charge transfer, diffusion processes, and the presence of protective films without significantly modifying the interface. Consequently, the parameters obtained from one technique can be used to support and validate the results of the other, reducing uncertainties, preventing misinterpretations, and offering a more comprehensive and consistent understanding of the material's corrosion behavior (Sheetal *et* al., 2023; Romaniv *et al.*, 1989).

Linear Potentiodynamic Polarization is based on the application of a potential range around the corrosion potential to describe the behavior of the resulting current variation. This behavior is governed by the Butler–Volmer equation, which is expressed in Equation 1 (Bard; Faulkner, 2000; Marshall, 2018; Romaniv *et al.*, 1989).

$$i = i_{corr}\left[\exp exp\left(\frac{\propto_a F\left(E-E_{corr}\right)}{RT}\right) - \exp exp\left(\frac{\propto_c F\left(E-E_{corr}\right)}{RT}\right)\right] \quad (1)$$

Where i_{corr} is the corrosion current (A), E is the applied potential (V), E_{corr} is the corrosion potential (V), α_a and α_c are the anodic and cathodic charge transfer coefficients, respectively, F is the Faraday constant (96485.33 C mol^{-1}), R is the ideal gas constant (8.314 J mol^{-1} K^{-1}), and T is the temperature (K). Equation 1 is also valid for current density responses, j (A cm^{-2}).

For small overpotentials ($|E - E_{corr}| \leq 30$ mV), the exponential terms in Equation 1 can be linearized, resulting in Equation 2 (Bard; Faulkner, 2000; Roberge, 1999).

$$i \approx i_{corr}\frac{F}{RT}\left(\propto_a + \propto_c\right)\left(E - E_{corr}\right) \quad (2)$$

Equation 2 represents the region in which the applied potential and the resulting current follow a linear relationship, allowing the graphical estimation of *Ecorr* and *icorr* values through the extrapolation of Tafel plots. These curves describe the electrode behavior under strong polarization, either anodic or cathodic, and are derived from Equation 1. Equations 3 and 4 correspond to the anodic and cathodic Tafel expressions, respectively (Bard; Faulkner, 2000; Roberge, 1999).

$$\log log \frac{i}{i_{corr}} = \left(\frac{\propto_a F}{2.303RT}\right)\left(E - E_{corr}\right) \quad (3)$$

$$\log log \frac{i}{i_{corr}} = \left(\frac{\propto_b F}{2.303RT}\right)\left(E - E_{corr}\right) \quad (4)$$

These equations provide the necessary information to determine the kinetic parameter *icorr*, which is required for calculating the corrosion rate using Equation 5 (ASTM INTERNATIONAL, 2015; Jones, 1995).

$$CR = \frac{K\, i_{corr}\, EW}{\rho} \quad (5)$$

Where *CR* is the corrosion rate (mm year^{-1}), *K* is a conversion constant, 3.27×10^{-3} (mm g μA^{-1} cm^{-1} year^{-1}), *EW* is the equivalent weight of the metal (equivalent-gram), and ρ is the metal density (g cm^{-3}).

EIS is based on measuring a system's resistance to the flow of alternating current over a given frequency range. This resistance is specifically referred to as impedance, which is expressed by Equation 6 (Hallemans *et al.*, 2023; Bard; Faulkner, 2000).

$$Z(\omega) = \frac{E(\omega)}{I(\omega)} \quad (6)$$

Where *Z* is the impedance (Ω), *E* denotes the electric potential (V), and *I* corresponds to the current (A). All of these variables are functions of ω, which represents the frequency of the alternating current. Another mathematical representation of impedance is given by Equation 7 (Hallemans *et al.*, 2023; Bard; Faulkner, 2000).

$$Z(\omega) = Z'(\omega) + jZ''(\omega) \quad (7)$$

In this representation, *Z'* correspond to the real part of the impedance, or the resistance of the circuit, and *Z''* represents the imaginary part, or the reactance of the circuit, representing the opposition to current flow due to the system's capacitance or inductance, and *j* is the imaginary unit ($\sqrt{-1}$).

The impedance of an electrochemical system is often represented by the Randles equivalent circuit model, as expressed in Equation 8. (Hallemans *et al.*, 2023; Bard; Faulkner, 2000).

$$Z(\omega) = R_s + \frac{1}{R_{ct} + j\omega C_{dl}} \quad (8)$$

Where *Rs* is the electrolyte resistance (Ω), *Rct* is the charge transfer resistance (Ω), and *Cdl* is the double-layer capacitance (F). The resistance and capacitance values in Equation 8 are obtained from Nyquist and Bode plots resulting from the application of the technique.

The Nyquist plot is a graphical representation of Equation 7, and when associated with a Randles circuit, it typically takes the form of a semicircle whose diameter corresponds to *Rct*, indicating the resistance of the electrode/solution interface to electron transfer in an electrochemical reaction (Lazanas; Prodromidis, 2025; Hallemans *et al.*, 2023; Bard; Faulkner, 2000).

Bode plots are curves that facilitate the interpretation of the system's behavior across a range of analyzed frequencies. One of these curves relates the phase angle (θ) to the logarithm of the frequency, allowing the evaluation of the coating or interfacial layer resistance based on the maximum magnitude

of θ and the frequency range over which this angle remains stable. The greater the layer resistance, the more stable θ remains with respect to frequency variation.

The other curve relates the impedance modulus (|Z|) to the logarithm of the frequency and provides information about the electrochemical processes involved, such as charge transfer, diffusion, and capacitive behavior. Comparatively, if a coating exhibits higher |Z| values than another, it indicates greater resistance to current flow (Bard; Faulkner, 2000; Walter, 1986).

3 Experimental

3.1 Preparation of Electrolytes

The solutions used in this study were prepared using analytical-grade reagents and distilled water. Table 1 shows the chemical composition of the Watts nickel bath used as a reference. Table 2 presents the compositions of the modified Watts electrolytes, characterized by the predominance of sulfate, chloride, and nitrate ions, respectively, prepared in stoichiometric proportions to maintain nickel ion concentrations equivalent to those of the reference bath in each case.

Table 1 – Chemical Composition of the Watts Electrolyte Used as Reference.

Componets	Concentration / mol L^{-1}
$NiSO_4 \cdot 6H_2O$	1.14
$NiCl_2 \cdot 6H_2O$	0.20
H_3BO_3	0.73

Source: (AHMAD, 2006)

Table 2 – Compositions of Electrolytes with Predominance of Chloride (1), Sulfate (2), and Nitrate (3) Ions.

Electrolytes	Components	Concentration / mol L^{-1}
1	$NiCl_2 \cdot 6H_2O$	1.34
	H_3BO_3	0.73
2	$NiSO_4 \cdot 6H_2O$	1.34
	H_3BO_3	0.73
3	$Ni(NO_3)_2 \cdot 6H_2O$	1.34
	H_3BO_3	0.73

Source: research data

3.2 Electrodeposition

Nickel electrodepositions were carried out in a conventional single-compartment Pyrex® glass cell with a total volume of 50 mL. The working electrodes were made of SAE 1020® carbon steel embedded in polyester resin, with an exposed circular geometric area of approximately 1.0 cm². A rectangular nickel plate (99.9% purity), with an approximate area of 6.4 cm² was used as the counter electrode.

Before the electrodeposition, the working electrodes were mechanically polished using silicon carbide papers of progressively finer grit sizes (220, 400, 600, 800, and 1200 mesh), followed by chemical degreasing in a 10% (w/v) NaOH solution and activation in a 10% (v/v) HCl solution. After each step, the electrodes were rinsed with distilled water.

Electrodeposition was performed in galvanostatic mode using a Metrohm Autolab® PGSAT204 potentiostat/galvanostat, with the electrodes positioned approximately 2.5 cm apart and applying a current density of 10 $A \cdot dm^{-2}$. The process was conducted for 15 minutes at 50 °C, pH 4.0, under constant stirring at 100 rpm, using a Teflon®-coated magnetic stir bar.

3.3 Deposited Masses and Cathodic Current Efficiencies

To measure the deposited masses, an analytical balance model AY220 from Shidmazu® with four-digit precision was used. The theoretical mass was calculated based on Faraday's law of electrolysis, as shown in Equation 9.

$$m = \frac{M\, i\, \Delta t}{n\, F} \quad (9)$$

Where m is the mass of nickel deposited (g), M is the molar mass of the element (g·mol^{-1}), i is the current used (A), n is the number of electrons involved in the reaction, F is Faraday's constant (96485.33 C·mol^{-1}), and t is the electrolysis time (s).

The cathodic current efficiency ($R(\%)$) was calculated using Equation 10.

$$R(\%) = \frac{m_d}{m_t} 100 \quad (10)$$

Where $R(\%)$ is the process efficiency (%), m_d is the deposited mass (g), and m_t is the theoretical mass previously calculated (g).

The coating thicknesses were calculated using Equation 11, as described by Dibari (2009).

$$E_D = \frac{m_d}{\rho A} \quad (11)$$

Where E_D is the thickness of the nickel deposit (cm), ρ is the density of nickel (g cm^{-3}), and A is the surface area of the electrode (cm²).

3.4 Scanning electron microscopy (SEM)

Surface images of the coatings were taken using Scanning Electron Microscopy (SEM) with a Tescan VEGA 3 microscope operated at an accelerating voltage 10 kV. The images were captured at magnifications of 1000x and 5000x.

3.5 Electrochemical corrosion tests

Electrochemical corrosion tests were conducted in an aqueous 3.0% NaCl solution using a three-electrode electrochemical cell. The setup consisted of an Ag/AgCl reference electrode, a platinum counter electrode, and a working electrode consisting of SAE 1020® steel coated with nickel.

Corrosion resistance was evaluated using linear polarization (LP) within a scanning range of ±300 mV with respect to the open-circuit potential (OCP), and electrochemical impedance spectroscopy (EIS) at OCP. Measurements were performed at room temperature over a frequency range from 10,000 Hz to 6 mHz. A 10-minute immersion period was applied prior to each measurement to ensure system stabilization. A Metrohm Autolab® PGSAT204 potentiostat/galvanostat was used to determine the corrosion parameters: corrosion rate (CR), corrosion potential (Ecorr), corrosion current density (jcorr), and charge transfer resistance (Rct) of the coatings.

4 Results and discussion

4.1 Electrodeposited mass, coating thickness, and cathodic current efficiency

Table 3 presents the experimental data for the electrodeposited mass, coating thickness, and cathodic current efficiency of the electrodeposits. In this table, the electrodeposits obtained from electrolytes 1, 2, and 3 (Table 2) are identified as ENC, ENS, and ENN, respectively.

Table 3 – Experimental Data of electrodeposited Masses, Thicknesses, and Cathodic Current Efficiencies of the Electrodeposits.

Electrodeposits	m_t / mg	m_d / mg	Thicknesses / µm	Efficiencies / %

ENC	31.5	30.7	30.0	97.52
ENS	31.5	29.4	29.0	93.39
ENN	31.5	9.3	9.0	29.54

Source: research data

The data in Table 3 show that ENS and ENC exhibited cathodic current efficiencies characteristic of nickel electrodeposits obtained from Watts-type solutions, which generally present values above 95% (Fukunaga; Ueda, 2024; Wojciechowski *et al.*, 2017; Rudnik, 2014; Ren *et al.*, 2012; Rusu *et* al., 2011; Taylor, 2001). In Comparison, the ENN samples showed lower cathodic current efficiency, probably because of the formation of intermediate species like $NiOH^{+}$. These species can move into the solution, taking Ni^{2+} ions with them and making it harder for the nickel to deposit on the surface (Navarro-Aguilar *et al.*, 2020; Muñoz; Salinas, 2003; Jayashree; Kamath, 2001; Streinz *et al*., 1995).

The coating thickness values shown in Table 3 are consistent with the corresponding cathodic current efficiencies and in agreement with data reported in the literature (Rusu *et* al., 2011). These results suggest that the nature of the anions present in the electrolyte exerts a significant influence on the nickel electrodeposition process.

4.2 Morphological analysis

All electrodeposits were adherent, uniform, and free from visually detectable defects or discontinuities. However, the ENN samples exhibited a matte and darker surface appearance compared to the others. Figure 1 shows the surface morphologies of the electrodeposits.

Figure 1 – Morphological analysis obtained by Scanning electron microscopy images: (a) ENC, 1000× magnification, (b) ENC, 5000× magnification, (c) ENS, 1000× magnification, (d) ENS, 5000× magnification, (e) ENN, 1000× magnification, and (f) ENN, 5000× magnification.

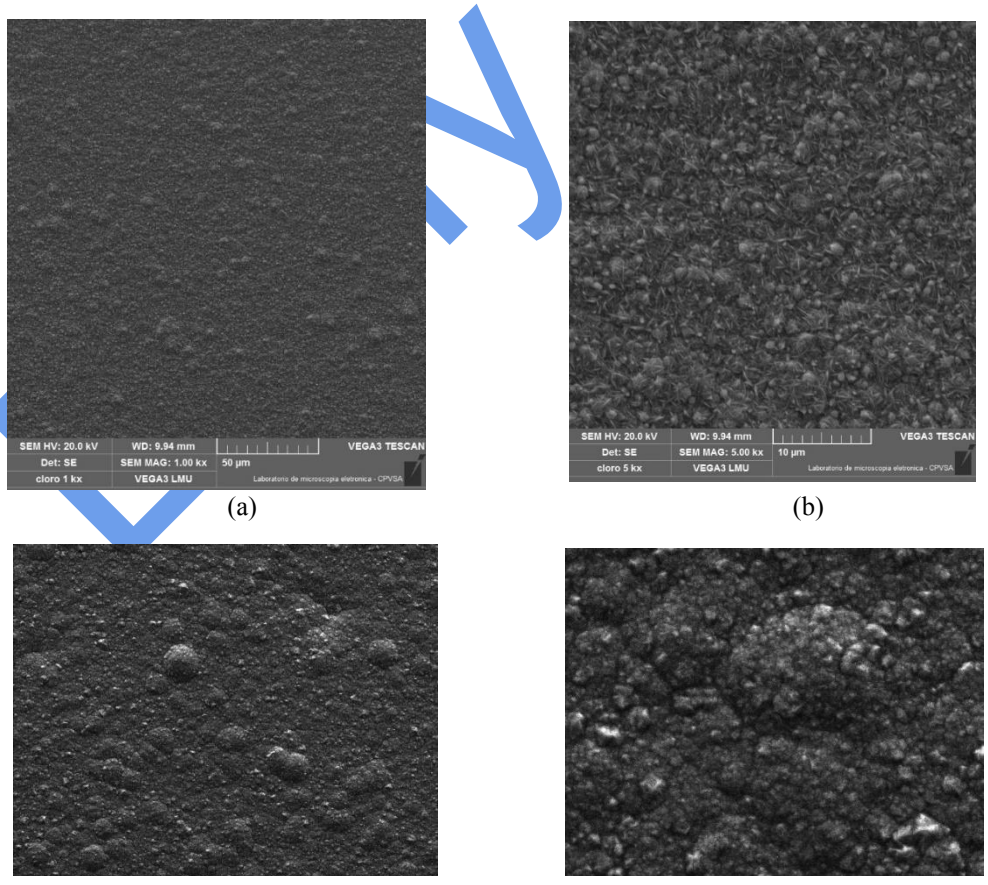

(a) (b)

(c) (d)

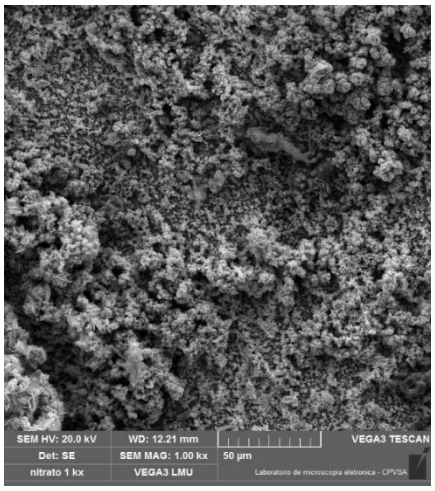

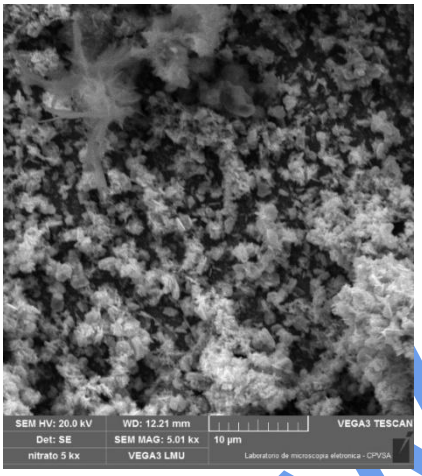

(e) (f)

Source: authors' archive

The micrographs shown in Figures 1a and 1b indicate that the ENC samples have a uniformly distributed nodular and dendritic surface morphology, typical of nickel electrodeposits. The presence of distinct morphologies suggests competitive growth of metal nuclei, even under conditions of uniform and controlled electrodeposition (Chat-Wilk *et al*., 2021; Karayannis & Patermarakis, 1995). This outcome is likely related to stable electrodeposition conditions influenced by current density and electrolyte composition, due to the presence of chloride ions.

Figures 1c and 1d, corresponding to the ENS samples, reveal a predominantly nodular surface morphology**,** with possible nodule coalescence resulting from the formation of comparatively larger nodules than those observed in the ENC samples (Mubshrah *et al*., 2024; Chat-Wilk *et al*., 2021; Karayannis & Patermarakis, 1995). This behavior suggests a lower nucleation rate or modifications in the electrolyte composition during electrodeposition, since sulfate anions do not promote anodic dissolution to the same extent as chloride anions.

Figures 1e and 1f show that the ENN samples present a porous surface morphology, with the presence of powdery material. This behavior is commonly observed in aqueous solutions containing nitrate ions (NO_3^-), which, through the action of water, are reduced to nitrite ions (NO_2^-) with the consequent release of OH^- ions, as demonstrated by several authors. This reaction leads to an increase in pH at the electrode–electrolyte interface during electrolysis, generating enough hydroxide to induce precipitation of $Ni(OH)_2$, even in buffered electrolytes and under moderately acidic bulk pH conditions (Sarangi et al., 2025; Navarro-Aguilar et al., 2020; E et al., 2016; Jayashree & Kamath, 2001; Murthy et al., 1996; Streinz et al., 1995).

4.3 Electrochemical Tests

Table 4 presents the experimental values of the corrosion potential (E_{corr}), corrosion current density (j_{corr}), charge transfer resistance (R_{ct}), and corrosion rate (CR) for the coatings.

Table 4 – Experimental Data Obtained from Electrochemical Tests.

Electrodeposits	E_{corr} / mV	j_{corr} / mA cm^{-2}	R_{ct} / Ω cm^2	CR / mm ano^{-1}
ENC	–403	0.0638	1079	1.375
ENS	–384	0.0076	1440	0.165
ENN	–706	0.2475	75	5.923

Source: research data

Figure 2 shows the LPP curves for the electrodeposits. The Ecorr and jcorr values were calculated from the intersection of the anodic and cathodic branches, using the Tafel extrapolation method.

Figure 2 – LPP curves for ENC (red), ENS (green), and ENN (blue) obtained in 3.0% NaCl solution at 25 °C.

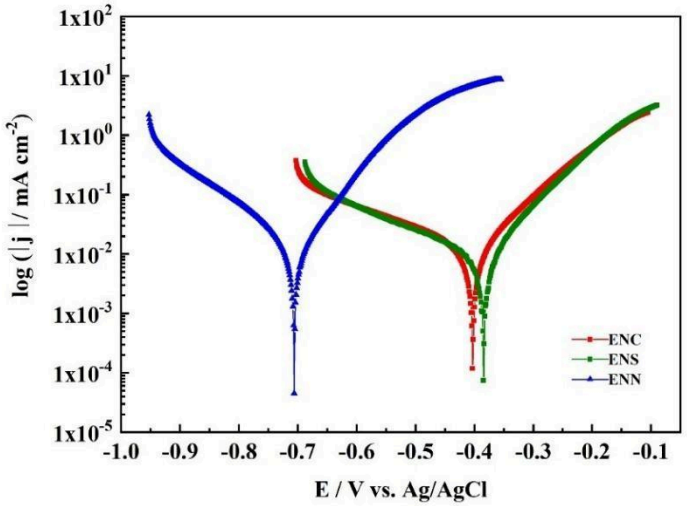

Source: research data

Figure 2 shows that the ENS and ENC samples exhibit more positive Ecorr values than the ENN, with the values listed in Table 4 typical of nickel coatings obtained from Watts formulations, which usually range between –760 and –220 mV (Basori *et al*., 2025; Sayed *et al*., 2022; Kucharska et al., 2016; Szeptycka *et al*., 2016; Ünal & Karahan, 2018; Rusu *et al*., 2011; Szczygieł & Kołodziej, 2005). These data indicate a more noble electrochemical behavior for ENS (–384 mV) compared to ENC (–403 mV), despite the relatively small difference between their corrosion potentials, and a substantially more positive potential than that observed for ENN (–706 mV).

The jcorr values in Table 4, in agreement with the Ecorr results, suggest a lower corrosion rate for ENS (0.0076 mA cm^{-2}) compared to ENC (0.0638 mA cm^{-2}) and ENN (0.2475 mA cm^{-2}). The higher corrosion kinetics observed for ENC in comparison with ENS were associated with its mixed nodular–dendritic surface morphology, since dendritic structures typically increase the electrochemically active surface area. The ENN samples exhibited the highest corrosion rate among the electrodeposits, which was attributed to their porous surface morphology. Thus, the most favorable corrosion performance was associated with ENS, whereas the least favorable performance was observed for ENN under the tested conditions.

Figure 3 presents the Nyquist plots obtained by electrochemical impedance spectroscopy for the electrodeposits.

Figure 3 – Nyquist plots for ENC (red), ENS (green), and ENN (blue) obtained in 3% NaCl solution at 25 °C.

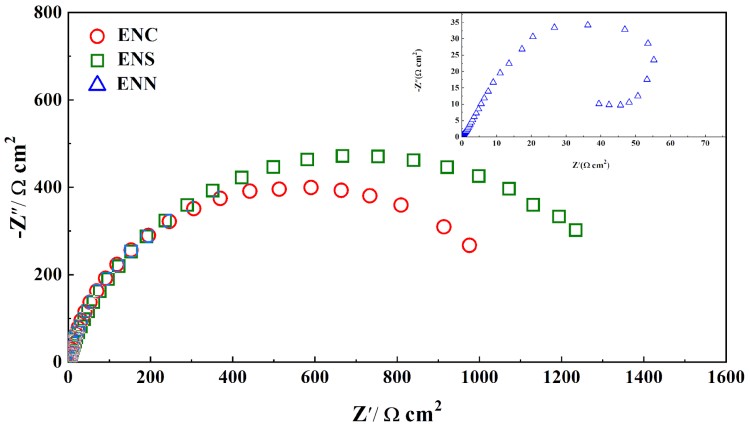

Source: research data

The figure shows a single capacitive arc for all samples. The Rct values for ENC and ENS are characteristic of nickel electrodeposits from Watts electrolytes (Rahimi *et al.*, 2025; Abbasi-Amandi et al., 2021; Shamshirsaz *et al.*, 2022; Rusu *et al.*, 2012; Mohajeri *et al.*, 2011) and have magnitudes of the same order: 1079 Ω·cm² and 1440 Ω·cm², respectively. ENN showed a much lower Rct value, with a magnitude of 75 Ω·cm².

The CR shown in Table 4 for ENS (0.165 mm year^{-1}), ENC (1.375 mm year^{-1}), and ENN (5.923 mm year^{-1}) are consistent with the previously presented jcorr and Rct values and support the corrosion resistance trends discussed above.

Figure 4 shows the Bode plots obtained by EIS for the electrodeposits: (a) phase angle and (b) impedance magnitude.

Figure 4 – Bode diagrams: (a) phase and (b) magnitude for ENC (red), ENS (green), and ENN (blue) obtained in 3.0% NaCl solution at 25 °C.

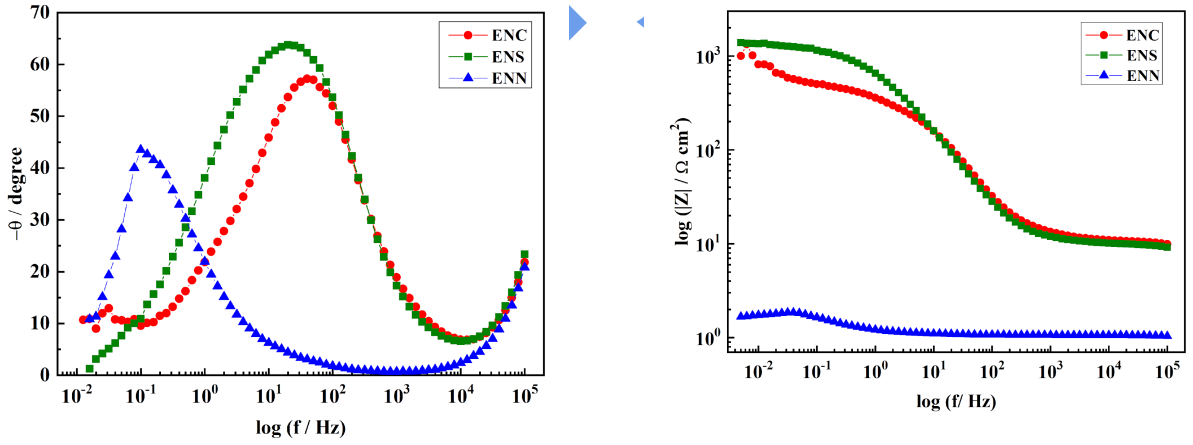

(a) (b)

Source: research data

Figure 4a reveals that ENS exhibited a phase angle (θ) of approximately 65°, with a broader and more stable phase-angle shifted toward lower frequencies when compared to ENC, which showed

θ of approximately 55°. The ENN displayed the lowest phase angle, around 42°, with a narrow peak at low frequencies. Figure 4b shows that at lower frequencies, ENS presented the highest impedance modulus (|Z|) values, while ENN exhibited the lowest |Z| values.

The data in Figure 4 are consistent with the Nyquist plots and LP curves, confirming the superior corrosion resistance of ENS compared to the other electrodeposits. These results are attributed to the influence of the predominant anions in the electrolytes, which was the main operational parameter varied in the experiments.

5 Conclusion

The experimental conditions used in this study were shown to be effective in producing nickel electrodeposits with good visual quality, uniform coverage, strong adhesion, and the absence of visible defects or discontinuities. It was observed that the predominant anions (Cl^-, SO_4^{2-}, and NO_3^-) in the electrolytes significantly influenced the cathodic current efficiency, surface morphology, and corrosion resistance of the coatings under the tested environment.

Chloride (Cl^-) anions provided greater electrolyte stability by maintaining the concentration of Ni^{2+} ions in solution. This is due to their ability to promote anodic corrosion, leading to high cathodic current efficiency, faster deposition rates, and the formation of a mixed nodular and dendritic surface morphology.

Sulfate (SO_4^{2-}) anions also resulted in high cathodic current efficiency, lower than that obtained with chloride, since they do not promote anodic corrosion or maintain electrolyte stability to the same extent. In contrast, nitrate (NO_3^-) anions significantly reduced cathodic current efficiency, likely due to simultaneous side reactions and the formation of nickel hydroxides, which resulted in porous and powdery deposits.

Thermodynamic and kinetic data from corrosion tests demonstrated that the surface morphology of the coatings directly affected their corrosion resistance. The Ecorr values showed that ENS coatings were more noble than ENC, which were more noble than ENN. Kinetic parameters jcorr and corrosion rate (CR) confirmed that ENS exhibited the lowest corrosion rate, followed by ENC and then ENN. Charge transfer resistance (Rct) values were consistent with these findings.

The analysis of the Bode plots corroborated the results obtained from linear polarization and impedance spectroscopy tests. ENS coatings exhibited the highest corrosion resistance, ENC coatings were slightly less resistant but still comparable, and ENN coatings showed the lowest resistance.

In summary, the type of anion present plays a key role in the electrodeposition process and determines the properties of the deposited coatings. This study provides useful insights for developing synthesis methods for nickel coatings and encourages further research on how different anions affect nucleation and growth mechanisms during electrodeposition, including the investigation of their microstructural features through X-ray Diffraction (XRD) analyses, thereby complementing the information beyond the scope addressed in this study.

Financial support

No significant financial support was received for this work that could have influenced its outcome.

Conflicts of interest

No conflicts of interest are disclosed.

Author Contributions

SILVA, G. P.: Conceptualization and study design; data collection, analysis, and/or interpretation; manuscript drafting and writing.

DANTAS, V. D.: Conceptualization and study design; data collection, analysis, and/or interpretation; manuscript drafting and writing.

SILVA FILHO, L. F.: Conceptualization and study design; data collection, analysis, and/or interpretation; manuscript drafting and writing.

SANTOS, Z. M.: Manuscript drafting and writing; critical revision with substantial intellectual contribution.

LIMA, R. N.: Manuscript drafting and writing; critical revision with substantial intellectual contribution.

BARROS NETO, E. L.: Manuscript drafting and writing; critical revision with substantial intellectual contribution.

References

ASTM INTERNATIONAL. **ASTM G102-89(2015)**: Standard Practice for Calculation of Corrosion Rates and Related Information from Electrochemical Measurements. West Conshohocken, Pennsylvania: Astm International, 2015. DOI: https://doi.org/10.1520/G0102-89R15E01.

ABBASI-AMANDI, Abolfazl; AHMADI, Naghi Parvini; OJAGHI-ILKHCHI, Mehdi; ALINEZHADFAR, Mohammad. Physical and electrochemical behavior of black nickel coatings in presence of KNO3 and imidazole additives. **Journal Of Electroanalytical Chemistry**, [S.L.], v. 893, p. 115310, jul. 2021. DOI: http://dx.doi.org/10.1016/j.jelechem.2021.115310.

AHMAD, Zaki. **Principles of Corrosion Engineering and Corrosion Control**. 1. ed. [S.L.]: Elsevier, 2006. DOI: https://doi.org/10.1016/B978-0-7506-5924-6.X5000-4. Accessed on:12 jan. 2025.

BARD, Allen J.; FAULKNER, Larry R.. **Electrochemical Methods: Fundamentals and Applications**. 2. ed. [S.L.]: Wiley, 2000. 864 p.

BASORI; MANSOR, Muhd Ridzuan; AJIRIYANTO, Maman Kartaman; KRISWARINI, Rosika; SOEGIJONO, Bambang; YUDANTO, Sigit Dwi; NANTO, Dwi; ROSYIDAN, Cahaya; SUSETYO, Ferry Budhi. Ni Layer Fabrication in Various Temperature of Watts Solution. **Journal of Applied Science of Engineering**, [S.L.], v. 28, n. 4, p. 853-864, 1 abr. 2025. DOI: http://dx.doi.org/10.6180/jase.202504_28(4).0016.

CHAT-WILK, Karolina; RUDNIK, Ewa; WŁOCH, Grzegorz; OSUCH, Piotr. Importance of anions in electrodeposition of nickel from gluconate solutions. **Ionics**, [S.L.], v. 27, n. 10, p. 4393-4408, 16 ago. 2021. DOI: http://dx.doi.org/10.1007/s11581-021-04166-y.

DENNIS, J.K.; SUCH, T.e.. Electroplating baths and anodes used for industrial nickel deposition. **Nickel And Chromium Plating**, [S.L.], p. 41-65, 1993. DOI: http://dx.doi.org/10.1533/9781845698638.41.

DIBARI, George A.. Nickel Plating. In: METAL Finishing: 76th Guidebook and Directory Issue. New York: Elsevier, 2009. p. 202-218. DOI: https://doi.org/10.1016/S0026-0576(00)80334-7

EL-HALLAG, Ibrahim; ELSHARKAWY, Safya; HAMMAD, Sherin. Electrodeposition of Ni nanoparticles from deep eutectic solvent and aqueous solution as electrocatalyst for methanol oxidation in acidic media. **International Journal Of Hydrogen Energy**, [S.L.], v. 46, n. 29, p. 15442-15453, abr. 2021. DOI: http://dx.doi.org/10.1016/j.ijhydene.2021.02.049.

E, Sharel P.; LIU, Danqing; LAZENBY, Robert A.; SLOAN, Jeremy; VIDOTTI, Marcio; UNWIN, Patrick R.; MACPHERSON, Julie V.. Electrodeposition of Nickel Hydroxide Nanoparticles on Carbon Nanotube Electrodes: correlation of particle crystallography with electrocatalytic properties. **The Journal Of Physical Chemistry C**, [S.L.], v. 120, n. 29, p. 16059-16068, 17 jun. 2016. American Chemical Society (ACS). DOI: http://dx.doi.org/10.1021/acs.jpcc.5b12741.

FUKUNAGA, Akihiko; UEDA, Shigetomo. Pulse electrodeposition of Ni–P alloy coatings from Watts baths: p content, current efficiency, and internal stress. **Electrochimica Acta**, [S.L.], v. 502, p. 144839, out. 2024. DOI :http://dx.doi.org/10.1016/j.electacta.2024.144839.

HALLEMANS, Noël; HOWEY, David; BATTISTEL, Alberto; SANIEE, Nessa Fereshteh; SCARPIONI, Federico; WOUTERS, Benny; LAMANTIA, Fabio; HUBIN, Annick; WIDANAGE, Widanalage Dhammika; LATAIRE, John. Electrochemical impedance spectroscopy beyond linearity and stationarity—A critical review. **Electrochimica Acta**, [S.L.], v. 466, p. 142939, out. 2023. DOI: http://dx.doi.org/10.1016/j.electacta.2023.142939.

JAYASHREE, R.s.; KAMATH, P.Vishnu. Nickel hydroxide electrodeposition from nickel nitrate solutions: mechanistic studies. **Journal Of Power Sources**, [S.L.], v. 93, n. 1-2, p. 273-278, fev. 2001. Elsevier BV. DOI: http://dx.doi.org/10.1016/s0378-7753(00)00568-1.

JONES, Denny A.. **Principles and Prevention of Corrosion**. 2. ed. Upper Saddle River, New Jersey: Pearson, 1995. 592 p.

LAZANAS, Alexandros Ch.; PRODROMIDIS, Mamas I.. Correction to “Electrochemical Impedance Spectroscopy─A Tutorial”. **Acs Measurement Science Au**, [S.L.], v. 5, n. 1, p. 156-156, 31 jan. 2025. DOI: http://dx.doi.org/10.1021/acsmeasuresciau.5c00007.

KUCHARSKA, Beata; BROJANOWSKA, Agnieszka; POPŁAWSKI, Karol; SOBIECKI, Jerzy Robert. Corrosion Resistance of Ni/Al2O3 Nanocomposite Coatings. **Materials Science**, [S.L.], v. 22, n. 1, p. 31-35, 18 fev. 2016. DOI: http://dx.doi.org/10.5755/j01.ms.22.1.7407.

MARSHALL, Aaron T.. Using microkinetic models to understand electrocatalytic reactions. **Current Opinion In Electrochemistry**, [S.L.], v. 7, p. 75-80, jan. 2018. DOI: http://dx.doi.org/10.1016/j.coelec.2017.10.024.

MOHAJERI, S.; DOLATI, A.; REZAGHOLIBEIKI, S.. Electrodeposition of Ni/WC nano composite in sulfate solution. **Materials Chemistry And Physics**, [S.L.], v. 129, n. 3, p. 746-750, out. 2011. DOI: http://dx.doi.org/10.1016/j.matchemphys.2011.04.053.

MUBSHRAH, Ayesha; MARTIN, Tomas; JONES, Christopher; SCHWARZACHER, Walther. Quantitative Analysis of Chloride Ion Influence on the Surface Morphology of Electrodeposited Polycrystalline Nickel Films. **Journal Of The Electrochemical Society**, [S.L.], v. 172, n. 3, p. 032504, 1 mar. 2025. DOI: http://dx.doi.org/10.1149/1945-7111/adbc26.

MUÑOZ, A.G,; SALINAS, D.R.. Inhibitory effects of NO^{2-} on Ni deposition. **Journal Of Electroanalytical Chemistry**, [S.L.], v. 547, n. 2, p. 115-124, maio 2003. DOI: http://dx.doi.org/10.1016/s0022-0728(03)00159-1.

MURTHY, Mahesh; NAGARAJAN, Gowri S.; WEIDNER, John W.; VAN ZEE, J. W.. A Model for the Galvanostatic Deposition of Nickel Hydroxide. **Journal Of The Electrochemical Society**, [S.L.], v. 143, n. 7, p. 2319-2327, 1 jul. 1996. The Electrochemical Society. DOI: http://dx.doi.org/10.1149/1.1837000.

NAVARRO-AGUILAR, A.I.; RUÍZ-GÓMEZ, M.A.; RODRÍGUEZ-GONZÁLEZ, V.; OBREGÓN, S.; VÁZQUEZ, A.. Effect of the Ni(NO3)2 additive on the electrophoretic deposition of NiO nanoparticles. **Ceramics International**, [S.L.], v. 46, n. 18, p. 28528-28535, dez. 2020. DOI: http://dx.doi.org/10.1016/j.ceramint.2020.08.010.

NICKEL INSTITUTE. **Nickel plating handbook**. [S.L.]: Nicke Institute, 2022. Available at: https://nickelinstitute.org/media/lxxh1zwr/2023-nickelplatinghandbooka5_printablepdf.pdf Accessed on: 12 jan. 2025.

OLIVEIRA, Francisco G.s.; SANTOS, Luis P.M.; SILVA, Rodolfo B. da; CORREA, Marcio A.; BOHN, Felipe; CORREIA, Adriana N.; VIEIRA, Luciana; VASCONCELOS, Igor F.; LIMA-NETO, Pedro de. FexNi(1-x) coatings electrodeposited from choline chloride-urea mixture: magnetic and electrocatalytic properties for water electrolysis. **Materials Chemistry And Physics**, [S.L.], v. 279, p. 125738, mar. 2022. DOI: http://dx.doi.org/10.1016/j.matchemphys.2022.125738.

ORIŇÁKOVÁ, Renáta; TUROňOVÁ, Andrea; KLADEKOVÁ, Daniela; GÁLOVÁ, Miriam; SMITH, Roger M.. Recent developments in the electrodeposition of nickel and some nickel-based alloys. **Journal Of Applied Electrochemistry**, [S.L.], v. 36, n. 9, p. 957-972, 14 jul. 2006. DOI: http://dx.doi.org/10.1007/s10800-006-9162-7.

RAHIMI, Ali; SARRAF, Shayan; SOLTANIEH, Mansour. The Effects of Soft Anodizing Pretreatments on the Corrosion Properties of Nickel Electroplated AA6061-T6. **Journal Of Materials Engineering And Performance**, [S.L.], p. 1-14, 17 fev. 2025. DOI: http://dx.doi.org/10.1007/s11665-025-10815-4.

REN, Xiu-Lian; WEI, Qi-Feng; LIU, Zhe; LIU, Jun. Electrodeposition conditions of metallic nickel in electrolytic membrane reactor. **Transactions Of Nonferrous Metals Society Of China**, [S.L.], v. 22, n. 2, p. 467-475, fev. 2012. DOI: http://dx.doi.org/10.1016/s1003-6326(11)61200-4.

ROMANIV, O. N.; TSIRUL'NIK, A. T.; KRYS'KIV, A. S.; RONCHEVICH, I. Ch.. Electrochemical methods in corrosion monitoring of metals (review). **Soviet Materials Science**, [S.L.], v. 25, n. 1, p. 1-12, 1989. Springer Science and Business Media LLC. http://dx.doi.org/10.1007/bf00727915.

RUDNIK, Ewa. Black Nickel Coatings: from plating techniques to applications. **Coatings**, [S.L.], v. 14, n. 12, p. 1588, 19 dez. 2024. DOI: http://dx.doi.org/10.3390/coatings14121588.

RUSU, D. E.; ISPAS, A.; BUND, A.; GHEORGHIES, C.; CÂRÂC, G.. Corrosion tests of nickel coatings prepared from a Watts-type bath. **Journal Of Coatings Technology And Research**, [S.L.], v. 9, n. 1, p. 87-95, 19 jul. 2011. DOI: http://dx.doi.org/10.1007/s11998-011-9343-0.

SAYED, Manal A. El; EL-HENDAWY, Morad M.; IBRAHIM, Magdy A.M.. Improving the Characteristics of Nickel Coatings Produced on Copper from Watts Bath in the Presence of Ascorbic Acid – Combined Experimental and Theoretical Study. **International Journal Of Electrochemical Science**, [S.L.], v. 17, n. 4, p. 22044, abr. 2022. DOI: http://dx.doi.org/10.20964/2022.04.12.

SARANGI, Chinmaya Kumar; ACHARY, G. Lilishree; SUBBAIAH, Tondepu; PARAMGURU, Raja Kishore; ROY, Sanat Kumar. Role of Electrochemical Precipitation Parameters in Developing Mixed-Phase Battery-Grade Nickel Hydroxide. **Electrochem**, [S.L.], v. 6, n. 1, p. 2, 16 jan. 2025. MDPI AG. DOI: http://dx.doi.org/10.3390/electrochem6010002.

SHAMSHIRSAZ, Mohsen; FEREIDOON, Abdolhosein; ALBOOYEH, Alireza; DANAEE, Iman. The Effect of Ni-Al2O3 Nanocomposite Coatings on the Wear and Corrosion Resistance and Thermal Diffusivity of 316 Stainless Steel Plates of Heat Exchangers. **Journal Of Materials Engineering And Performance**, [S.L.], v. 32, n. 4, p. 1529-1544, 29 ago. 2022. DOI: http://dx.doi.org/10.1007/s11665-022-07242-0.

SZCZYGIEŁ, Bogdan; KOŁODZIEJ, Małgorzata. Composite Ni/Al2O3 coatings and their corrosion resistance. **Electrochimica Acta**, [S.L.], v. 50, n. 20, p. 4188-4195, jul. 2005. DOI: http://dx.doi.org/10.1016/j.electacta.2005.01.040.

JAYASHREE, R.s.; KAMATH, P.Vishnu. Nickel hydroxide electrodeposition from nickel nitrate solutions: mechanistic studies. **Journal Of Power Sources**, [S.L.], v. 93, n. 1-2, p. 273-278, fev. 2001. DOI: http://dx.doi.org/10.1016/s0378-7753(00)00568-1.

PESQUEIRA, Camila Melo; LUIZ, Leonardo Augusto; ANDRADE, Juliano de; GARCIA, Carlos Mario; PORTELLA, Kleber Franke. The effect of chloride, sulfate, and ammonium ions on the semiconducting behavior and corrosion resistance of AISI 304 stainless steel passive film. **Matéria (Rio de Janeiro)**, [S.L.], v. 28, n. 4, p. 1-10, out. 2023. DOI: http://dx.doi.org/10.1590/1517-7076-rmat-2023-0139.

RAHIMI, Ali; SARRAF, Shayan; SOLTANIEH, Mansour. The Effects of Soft Anodizing Pretreatments on the Corrosion Properties of Nickel Electroplated AA6061-T6. **Journal Of Materials Engineering And Performance**, [S.L.], p. 1-15, 17 fev. 2025. DOI: http://dx.doi.org/10.1007/s11665-025-10815-4.

ROMANIV, O. N.; TSIRUL'NIK, A. T.; KRYS'KIV, A. S.; RONCHEVICH, I. Ch.. Electrochemical methods in corrosion monitoring of metals (review). **Soviet Materials Science**, [S.L.], v. 25, n. 1, p. 1-12, 1989. DOI: http://dx.doi.org/10.1007/bf00727915.

RUDNIK, Ewa. The influence of sulfate ions on the electrodeposition of Ni–Sn alloys from acidic chloride–gluconate baths. **Journal Of Electroanalytical Chemistry**, [S.L.], v. 726, p. 97-106, jul. 2014. DOI: http://dx.doi.org/10.1016/j.jelechem.2014.05.021.

RUSU, D. E.; ISPAS, A.; BUND, A.; GHEORGHIES, C.; CÂRÂC, G.. Corrosion tests of nickel coatings prepared from a Watts-type bath. **Journal Of Coatings Technology And Research**, [S.L.], v. 9, n. 1, p. 87-95, 19 jul. 2011. DOI: http://dx.doi.org/10.1007/s11998-011-9343-0.

SHEETAL; KUNDU, Sheetal; THAKUR, Sanjeeve; SINGH, Ashish Kumar; SINGH, Manjeet; PANI, Balaram; SAJI, Viswanathan S.. A Review of Electrochemical Techniques for Corrosion Monitoring – Fundamentals and Research Updates. **Critical Reviews In Analytical Chemistry**, [S.L.], v. 55, n. 1, p. 161-186, 25 out. 2023. DOI: http://dx.doi.org/10.1080/10408347.2023.2267671.

STREINZ, Christopher C.; HARTMAN, Andrew P.; MOTUPALLY, Sathya; WEIDNER, John W.. The Effect of Current and Nickel Nitrate Concentration on the Deposition of Nickel Hydroxide Films. **Journal Of The Electrochemical Society**, [S.L.], v. 142, n. 4, p. 1084-1089, 1 abr. 1995. DOI: http://dx.doi.org/10.1149/1.2044134.

SZEPTYCKA, Benigna; GAJEWSKA-MIDZIALEK, Anna; BABUL, Tomasz. Electrodeposition and Corrosion Resistance of Ni-Graphene Composite Coatings. **Journal Of Materials Engineering And Performance**, [S.L.], v. 25, n. 8, p. 3134-3138, 23 mar. 2016. DOI: http://dx.doi.org/10.1007/s11665-016-2009-4.

TAYLOR, S.R.. Coatings for Corrosion Protection: metallic. **Encyclopedia Of Materials**: Science and Technology, [S.L.], p. 1-5, 2001. DOI: http://dx.doi.org/10.1016/b0-08-043152-6/00239-4.

ÜNAL, E.; KARAHAN, İ.H.. Production and characterization of electrodeposited Ni-B/hBN composite coatings. **Surface And Coatings Technology**, [S.L.], v. 333, p. 125-137, jan. 2018. DOI: http://dx.doi.org/10.1016/j.surfcoat.2017.11.016.

WALTER, G.W.. A review of impedance plot methods used for corrosion performance analysis of painted metals. **Corrosion Science**, [S.L.], v. 26, n. 9, p. 681-703, jan. 1986. DOI: http://dx.doi.org/10.1016/0010-938x(86)90033-8.

WANG, Dongai; LI, Feihui; SHI, Yan; LIU, Meihua; LIU, Bin; CHANG, Qing. Optimization of the Preparation Parameters of High-Strength Nickel Layers by Electrodeposition on Mild Steel Substrates. **Materials**, [S.L.], v. 14, n. 18, p. 5461, 21 set. 2021. DOI: http://dx.doi.org/10.3390/ma14185461.

WOJCIECHOWSKI, Jarosław; BARANIAK, Marek; PERNAK, Juliusz; LOTA, Grzegorz. Nickel Coatings Electrodeposited from Watts Type Baths Containing Quaternary Ammonium Sulphate Salts. **International Journal Of Electrochemical Science**, [S.L.], v. 12, n. 4, p. 3350-3360, abr. 2017. DOI: http://dx.doi.org/10.20964/2017.04.70.